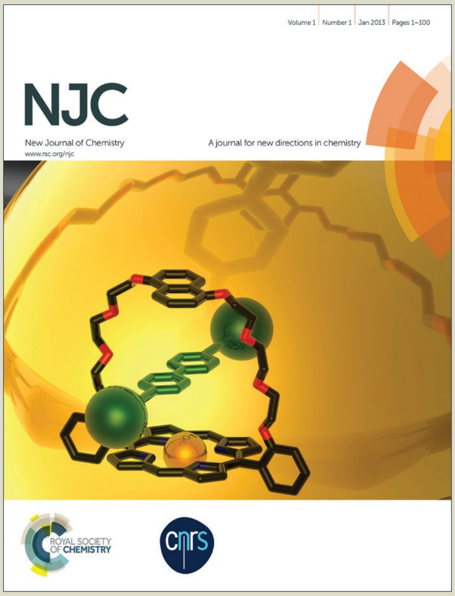
Volume 1 | Number 1 | Jan 2013 | Pages 1–100
NJC
New Journal of Chemistry
www.rsc.org/njc
A journal for new directions in chemistry
ROYAL SOCIETY OF CHEMISTRY
cnrs

New Journal of Chemistry

ARTICLE

Molecular Dynamic Simulations of Core-Shell Microsphere of Nanosilica Grafted by Acrylamide Acrylicacid Copolymer PAMAA: Study of Its Microstructure and Interaction Between Microsphere and additives

Received 00th January 20xx,
Accepted 00th January 20xx

DOI: 10.1039/x0xx00000x

www.rsc.org/

Shanshan Dai[a,b,*], Jinghan Zhang[a], Tailiang Zhang[a], Zhiyu Huang[a] Hongping Quan[a] Hongsheng Lu[a] Xiaowen Zhao[c]

Nanosilica grafted by acryl amide (AM) acrylic acid (AA) copolymer (PAMAA) is designed in this work to make functional material where nano-SiO_2 provides the rigidity and strength, and the copolymer the elasticity and flexibility. The resulting microsphere with core-shell structure is able to enter, expand, shut off and remove in the deep layers of oilfield. Qualitative results can be easily obtained from normally experimental methods, but lots of quantitative relationships are still missing. To solve the problem mentioned above, molecular dynamic (MD) simulation is applied in this work to study the microstructure of microsphere and interaction between microsphere and additives. Aqueous solution (S1), solutions with sodium dodecyl sulfate (SDS, S2), dodecyl trimethyl ammonium bromide (DTAB, S3), and alcohol ethoxylate (AEO, n=3, S4) are built, and then the non-bond energy, radius of gyration (ROG) of microsphere, radial distribution function (RDF) for microsphere-additive pairs and mean square displacement (MSD) of polymer chains in these 4 different solutions are calculated in 325K, 350K and 375K respectively. Results show that addition of surfactants leads to a more stretching structure of the polymer chain. The hydration effect and mobility of polymer chain increase in both aqueous and surfactant solutions as temperature increases.

1. Introduction

With the rapid advancement of manufacturing techniques for nano-structured materials, polymer/ inorganic composite that contain nanosized fillers have received considerable attention recently.[1-6] Behind the potential applicability of these composites are their expected multifunctionality and the onset of unusual properties originated from the structural ordering and densification of the matrix polymer in the vicinity of the inorganic fillers.[7,8] For example, a Fe_3O_4 nanoparticle grafted by poly(2-vinyl-4,4-dimethylazlactone) was employed as an effective template *l*-asparaginase immobilization.[9] The rubber industry widely employs carbon black and silica particles of a wide size distribution as reinforcing fillers which increases tire strength and toughness while also improving the rubber's resistantce to tearing, abrasion, and flex fatigue.[10] A series of SiO_2-polyaniline core-shell microspheres with an ultrathin conducting over layer are applied as the sensor for ascorbic acid replacing conducting polymers.[11] Poly(*p*-vinylphenylsulfonylhydrazide) graft silica, which was toughened, strengthened and stiffened simultaneously, can significantly improve the notch impact strength of polypropylene when they are blended.[12]

It is therefore possible and advantageous to combine the excellent properties of different materials. In this work, nanosilica grafted by acryl amide (AM) acrylic acid (AA) copolymer (PAMAA) is designed in this work to make functional material where nano-SiO_2 provides the rigidity and strength, and the copolymer the elasticity and flexibility. The resulting microsphere with core-shell structure is able to enter, expand, shut off and remove in the deep-layers of oilfield. Qualitative results can be easily obtained from normally experimental methods, but lots of quantitative relationships are still missing. To solve the problems mentioned above, molecular dynamic (MD) simulation provides the most detailed look at the nature of micro-sized events in the interface and interphase regions is lead to the design of more accurate experiments and better data interpretation in this work. For its chemical rigorousness and usefulness in describing behaviours of condensed matters, the MD simulation has been widely used to predict the properties of polymer materials and local interaction problem of material interface recently.[13-21] Researches find that grafted density, surface curvature of nanoparticles have great effects on the morphologies of polymer chains. Works by the Tinashe V. M. Ndoro[20] indicate that at low grafted density, the grafted chains near the surface are not always stretched but rather show a small radius of gyration. And with

---

[a] *College of Chemistry and Chemical Engineering, Southwest Petroleum University, Chengdu 610500, Sichuan, China.*
Email: ashanscu@163.com
[b] *Oil& gas Field Applied Chemistry Key Laboratory of Sichuan Province, Chengdu 610500, Sichuan, China.*
[c] *State Key Laboratory of Polymer Materials Engineering, Polymer Research Institute of Sichuan University, 610065 Chengdu, China*

reduced curvature, the grafted chains close to the surface have a tendency to become more stretch. Hossein Eslami[21] compared the monomer density of grafted chains and free chains from the microparticle surface. The results show that the density peaks of monomer for the grafted chains are more pronounced in systems with bigger microparticles. On the contrary, the peaks for free chains are more obvious in systems with smaller microparticles. Hua Liu[22] reports a study of MD simulation on cadmium sulfide microparticles grafted by polymers with different groups. The results of interaction between the polymers and microparticles show that the absence of alkyl side chains decrease the distance of conjugated backbones from the surface, polymers with terminal hydroxyl groups on alkyl side chains approach the surfactant corona while ester groups bound to aromatic rings in the poly (phenyleneethynylene) backbone cannot. In the most actual conditions, microspheres are in solutions, such as microspheres dispersed in liquid coating can improve the stability of the coating and microspheres combined with surfactant as plugging agent are usually in pure or brine water. But so far, there are few researches on the interaction between the microspheres and solution, or the morphologies of microspheres in the solution due to its complexity, which is so important to further study the relationship between structure and properties of these microsphere systems. Unfortunately, the relatively mechanisms are still unknown and the results obtained from the traditional experiments are difficultly for further study at a molecular level. Therefore, aqueous solution (S1), solutions with sodium dodecyl sulfate (SDS, S2), dodecyl trimethyl ammonium bromide (DTAB, S3), and alcohol ethoxylate (AEO, n=3, S4) are built in this simulation, and then the non-bond energy, radius of gyration (ROG) of microsphere, radial distribution function (RDF) for microsphere-additive pairs and mean square displacement (MSD) of polymer chains in these 4 different solutions are calculated in 325K, 350K and 375K respectively.

1. Models

A commercially available MD simulation package Material Studio 4.0 (Accelrys Inc., San Diego, CA) installed on Windows 7 with the DREIDING force field for inter- and intra- atomic interactions was used in this work, and the overall molecular modeling and simulation methodology are described as a flow chart shown in Fig. 1.

A nanosilica particle with radius of 0.5nm was trimmed from the α-quartz[23] in the form of sphere. The corresponding parameters of α-quartz are: a=4.909996, b=4.909996, c=5.402; All of the free radicals of the spherical nanosilica atoms lying outside of the spherical surface are first treated by oxygen atoms to mimic the real oxidation process, and oxygen atoms are saturated by hydrogen atoms. Then chains of AM-AA copolymer consist of 10 repeating units have been built, whose monomer ratio is 1:1, and they are minimized by smart method for 2000 iterations (structure of monomers and single copolymer chain are shown in Fig. 2.). To generate polymer grafted microsphere, hydrogen atoms on the silica surface were chosen and copolymer chains were grafted to the silica surface oxygen atoms via the end carbon atoms of the PAMAA. In this paper, 15 hydrogen atoms are randomly chosen to graft. Works of Seunghwa Yang[24] and Hossein Eslami[21] are partially considered as references to the method of molecular modeling mentioned above.

The resulting microspheres are minimized from coarse convergence tolerance (2×10^{-3} kcal/mol) to fine convergence tolerance (10^{-4} kcal/mol) by 5000 steps for 3 times. To search the optimal conformation, an annealing dynamic simulation was also performed on this structure. The corresponding processes are 5 repeated temperature cycles (from 350K to 700K and back) using constant volume/constant temperature (NVT) MD conditions. At the end of each annealing cycle, the structures were again energy minimized to convergence tolerance below 10^{-4} kcal/mol. Only the structure corresponding to the minimum energy will be used for further modeling. The structures before and after annealing treatment are both shown in Fig. 3.

Three surfactants, SDS, DTAB, and AEO are built by sketch tool, and then minimized respectively. The corresponding molecules are as shown in Fig. 4.

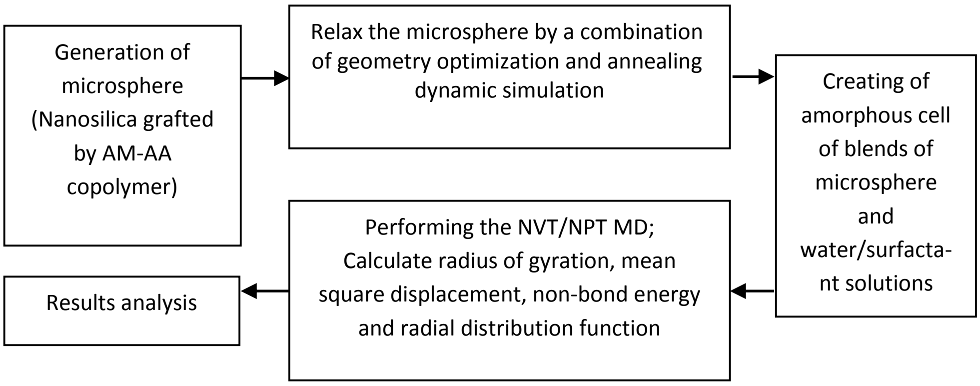

Fig. 1 The flow chart of simulation process.

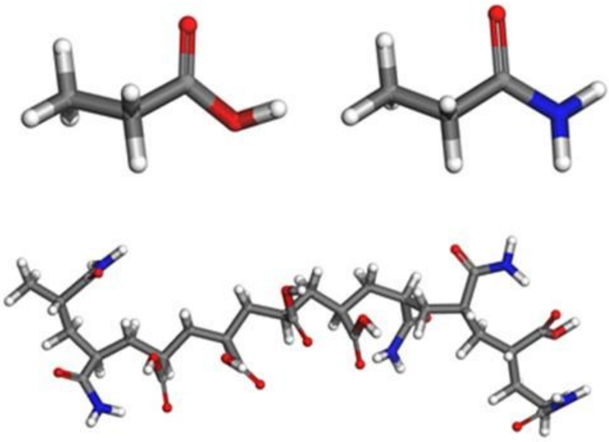

Fig. 2 Structure of AA, AM and single copolymer chain. (Gray refer to carbon atoms, white hydrogen, red oxygen, blue nitrogen.)

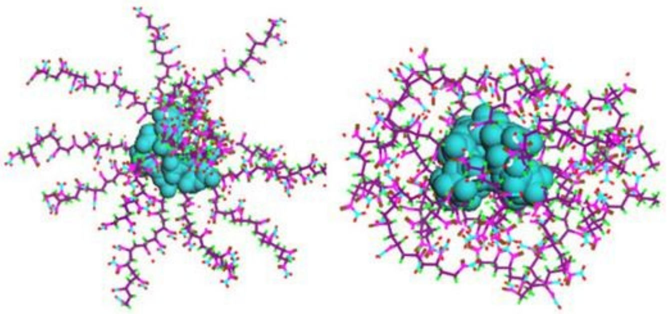

Fig. 3 Snapshots of grafted microspheres before (left) and after (right) annealing treatment.

Table 1 Simulation details of microsphere system

Microsphere system	Category and number of surfactants	Total number of atoms	number of H_2O molecules	Number of microspheres	Cell size （Å）	Cell density (g/cm^3)
S1	0	4400	982	1	37.3×37.3×37.3	0.6
S2	SDS 7	4701	982	1	38.5×38.5×38.5	0.6
S3	DTAB 6	4706	982	1	38.5×38.5×38.5	0.6
S4	AEO 6	4760	982	1	38.5×38.5×38.5	0.6

2. Simulation details

Four periodic unit cells are built as follow: One cell is loaded with a microsphere in aqueous solution. Other three cells are loaded with a microsphere in SDS, DTAB, and AEO solutions respectively. Each centroid of microsphere in these 4 systems is located in the centre of cell. Cell density is 1.2g/cc, and the corresponding cell size is 35Å×35Å×35Å. All the parameters are listed in Table 1.

A 2ns of NVT ensemble dynamic simulation at 325K was followed after constructing the periodic unit cells mentioned above. When microsphere systems reached an initial equilibration, in continuation of the simulation, an 8ns of NPT ensemble dynamic simulation is applied on these cells at 325K, 350K, 375K and 1atm to achieve final equilibrium t energy and temperature. The trajectory obtained in the last 4ns in NPT dynamic simulation process is chosen to do the analysis. Simulations used Dreiding[25], an all-atom forcefield, which has good coverage for organic, biological and main group of inorganic molecule. Dreiding forcefield is a purely diagonal forcefield with harmonic valence and cosine Fourier expansion torsion terms. The van der Waals interactions are described by the Lennard-Jones 12-6[26] type expression. Electrostatic interactions are described by atomic monopoles and a screened (distance-dependent) coulombic term. Hydrogen bonding is described by an explicit Lennard-Jones 12-10 potential[25]**.** It is worth noting that the Dreiding forecefield cannot assign charges automatically, charge parameters were assigned according to the compass forcefield. Charge parameters of compass forcefield are calculated by the quantum mechanics[27], which improves the accuracy of the calculation obviously. The time step of 1.0fs and Velocity Verlet algorithm[28] are adopted for the integration of atom motion equation in all simulations. The temperature and pressure are kept cnstant by controlling the system to a Nose thermostat[29] and Berendsen barostat[30]. The non-bonded interactions include Vander Waals potential energy, coulomb energy, and hydrogen bond energy. Atom-based was used for the Vander Waals potential energy with a cut-off of 1.25nm, Ewald[31] method was used for Coulomb interactions, and Atom based method is chosen for the hydrogen bond interaction with a cutoff of 0.45nm. Energies and other statistical data (coordinates, velocities, and forces) were stored every 5000 steps during the simulation. The snapshots of final structure at each temperature are shown in Fig.5.

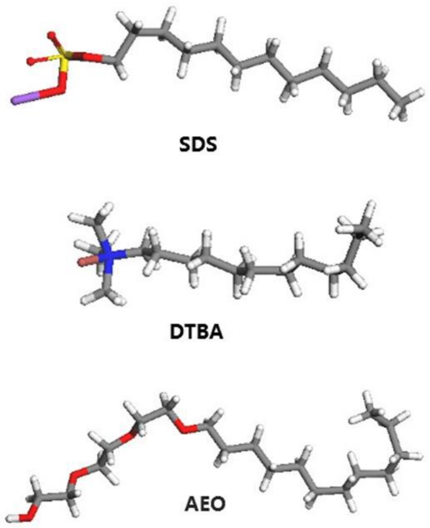

Fig. 4 Snapshots of surfactant molecules. (Gray refer to carbon atoms, white hydrogen, red oxygen, blue nitrogen, yellow sulfur, purple sodium and brown bromine).

The initial structure in vacuum, after annealing dynamic treatment shown in Fig.3, nanosilicas wrapped by copolymer chains forming a completely spherical structure of core-shell. Compared this initial structure, nanosilica is also wrapped by molecular chains of copolymer in aqueous or surfactant solutions as shown in Fig. 5, but the molecular chains of copolymer do not totally bend toward the core. The copolymer chains are partly get rid of the constraint of the SiO_2 core. These copolymer chains get fluffier, especially in surfactant solutions, copolymer chains are apparently stretched outward and around with the surfactants molecules. The corresponding quantitative analysis will be mentioned in the part of results and discussion.

4. Results & Discussion

4.1 Non-bond Energy of System.

Non-bond energy of system composed of hydrogen bond, the coulomb electrostatic, van der Waals contributions of each system at various temperature was shown in Fig. 6. The change of electrostatic interaction is much stronger than hydrogen bond and van der Waals in all four systems at all the calculating temperature. Therefore, electrostatic interactions play an important role on the structure of microsphere. Fig. 6 also show that electrostatic, van der Waals and hydrogen bond interactions are enhanced by adding the surfactant molecules, mainly due to the increase of interactions between the copolymer chains and surfactant molecules. The coulomb electrostatic energy of S2 system at the three temperatures are greater than the other systems, illustrating the addition of SDS greatly promote greater electrostatic interaction in these systems. In the same system, the hydrogen bond interaction decrease with the increase of the temperature, because of the weakened hydrogen bond interactions.

4.2 Radius of Gyration of Microsphere (ROG).

Radius of Gyration refers to molecular size of polymer. In general, lower values indicate bending of the linear molecular geometry.

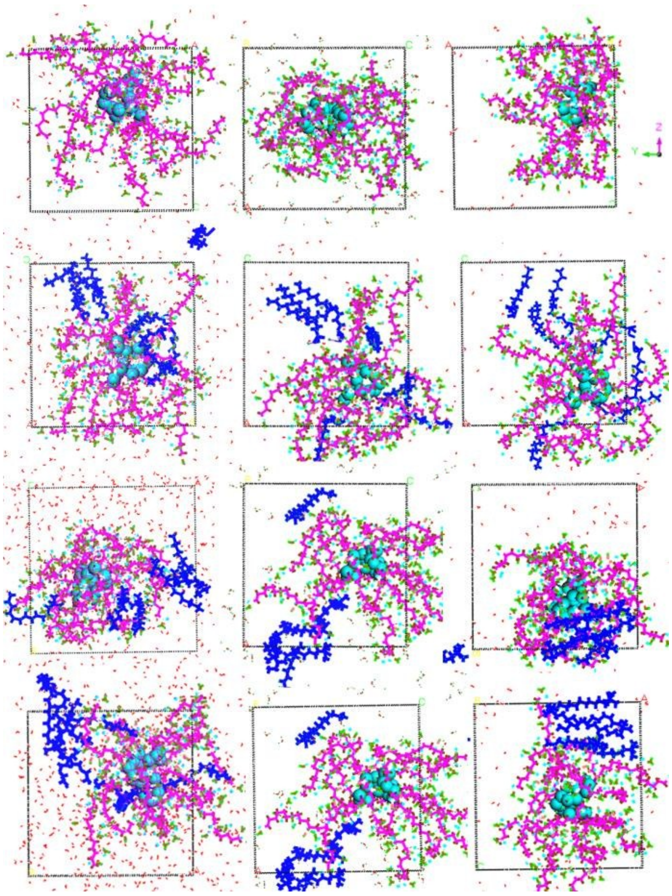

Fig. 5 Snapshots of dynamic equilibrium structure of system S1, S2, S3, and S4 (from top to bottom) at 325K, 350K, and 375K (from left to right). (Green balls refer to the SiO2 microsphere, red lines the polymer chains, blue lines surfactant molecules, and the dots around them H2O molecules).

As shown in Fig. 7, the radius of gyration of S2, S3, and S4 are greater than S1 system at all the three different temperatures. Namely, the addition of SDS, DTAB and AEO is of benefit to the stretch of the copolymer chains, and the instantaneous visualizations in Fig. 5 also reveal this phenomenon. In S1 system, the value of ROG reduces with the increase of temperature, it is due to the broken hydrogen bonds at high temperature. In S2 system, SDS that ionize into negative charge have an electric repulsion with the polymer negatively charged, which makes chains more stretched than in S1 system. In S3 system, compared with 325K, the coulombic force between the cationic surfactant DTAB and polymer is enhanced at 350K, and the polymer chains more stretch. ROG of S3 system at 375K are obviously reduced, due to the bad thermal stability of DTAB. In addition, ROG of microsphere in S4 system are greater than other system at 375K. It is supposed to be the effect of hydrophobic interaction on the radius of gyration, and the high temperature promote the hydrophobic interaction.

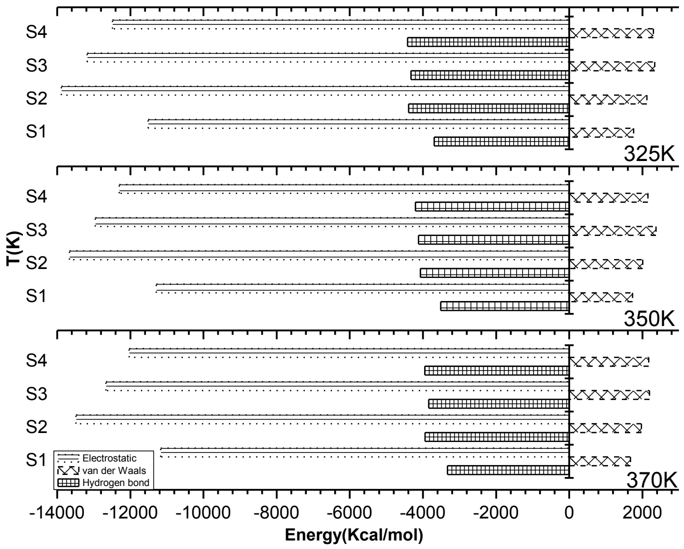

Fig. 6 Electrostatic, Vander Waals, hydrogen bond energy of S1, S2, S3, and S4 system at 325K, 350K, 375K.

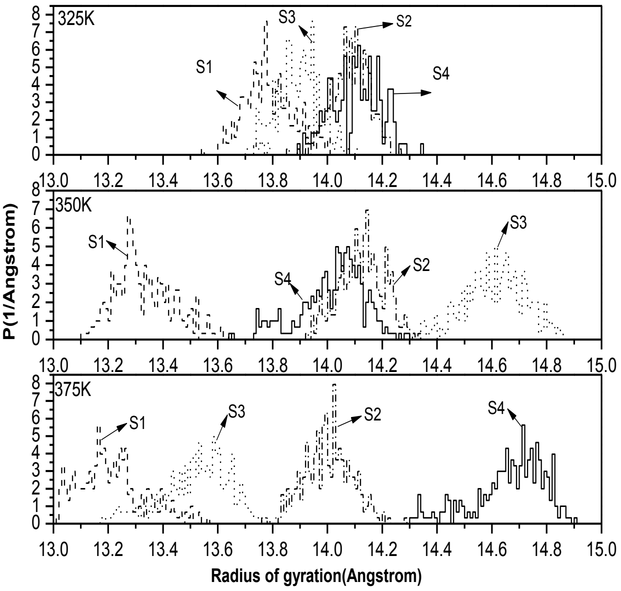

Fig. 7 The radius of gyration of S1, S2, S3, and S4 system at 325K, 350K and 375K respectively. (Vertical coordinate P is the probability density at this point).

4.3 Radial Distribution Function (RDF).

The interaction between solvent molecules and polymer chains has a significant effect on the morphology and properties of the microsphere. In order to analyse the effect of the water and surfactant molecules on the chains conformation in each system, the radial distribution function for microsphere-water and microsphere-surfactant pairs are calculated. Besides, the RDF of oxygen atoms in carboxyl groups of copolymer-oxygen atoms of water and the nitrogen atoms in amide groups of copolymer-oxygen atoms of water pairs are also calculated, for the further study of hydrogen bond. As is shown in Fig. 8, the radial distribution function for microsphere-water pair in S1, S2, S3 and S4 systems. There are two sharp peaks and one shoulder peak in all 4 systems at three different temperatures. The shape peaks basically appear at the same distance, which suggests the main three hydration points are at the same position. All the values of peaks in four systems become lower with the increase of temperature, which is in accord with the energy of hydrogen bond shown in Fig. 6. It is illustrated that high temperature breaks hydrogen bonds. In addition, the value of sharp peaks are greater in surfactant solutions compared with in aqueous solution at the same temperature, which means the hydration of microsphere in surfactant solutions is greater than in water solution, namely, addition of surfactants promote hydration effect. Compared the value of RDF of microsphere-water with the ROG of microsphere at different temperature for S1 system, the hydration degree enhanced with the increase of ROG of microsphere. It illustrate that stretched chains has a better hydration effect that result from the more stretched chains can increase the contact area with more hydrogen bonds formed. But this rule cannot applied to the other three system. For example, the hydration degree of microsphere for S4 system at 325K are better as compared to 350K, but the stretched degree is opposite. This means that the factors affecting the structure of microsphere are not only hydrogen but also interaction between surfactant molecules and microsphere. As shown in Fig. 9, the interaction between microsphere and surfactant molecules is explained to a remarkable effect on the structure of microsphere, so the radial distribution function of microsphere-surfactant pair are calculated in Fig. 9. Radial distribution function of microsphere-surfactant pair in S2 system shows a first sharp peak appeared at a distance of 1.5Å, a shoulder peak around 6Å and a shoulder peaks around 8 Å at 325K, and peaks at 350K and at 375K show a significant delay and peaks became wider, the first peak appears around 6.8 Å. But the height of peak did not become weaker with increase of temperature. This show that surfactants became farther from the centre of microsphere with increase of temperature, it indicated that a lot of interaction sites formed on the copolymer chains and surfactant molecules are uniformly interacted. In S3 system, the peak appears at 6.3 Å at 325K, but nearly no peaks at 350K and 375K. It indicated that temperature has a great effect on interaction between surfactants and microsphere in S3 system due to the bad thermostability of cationic surfactants. In S4 systems, peaks became wider with the increase of temperature, but height of peaks have no obvious change. It indicated that chains became more stretched with increase of temperature. The more stretched polymer chains leading the surfactants can be interacted with polymer chains more homogeneously.

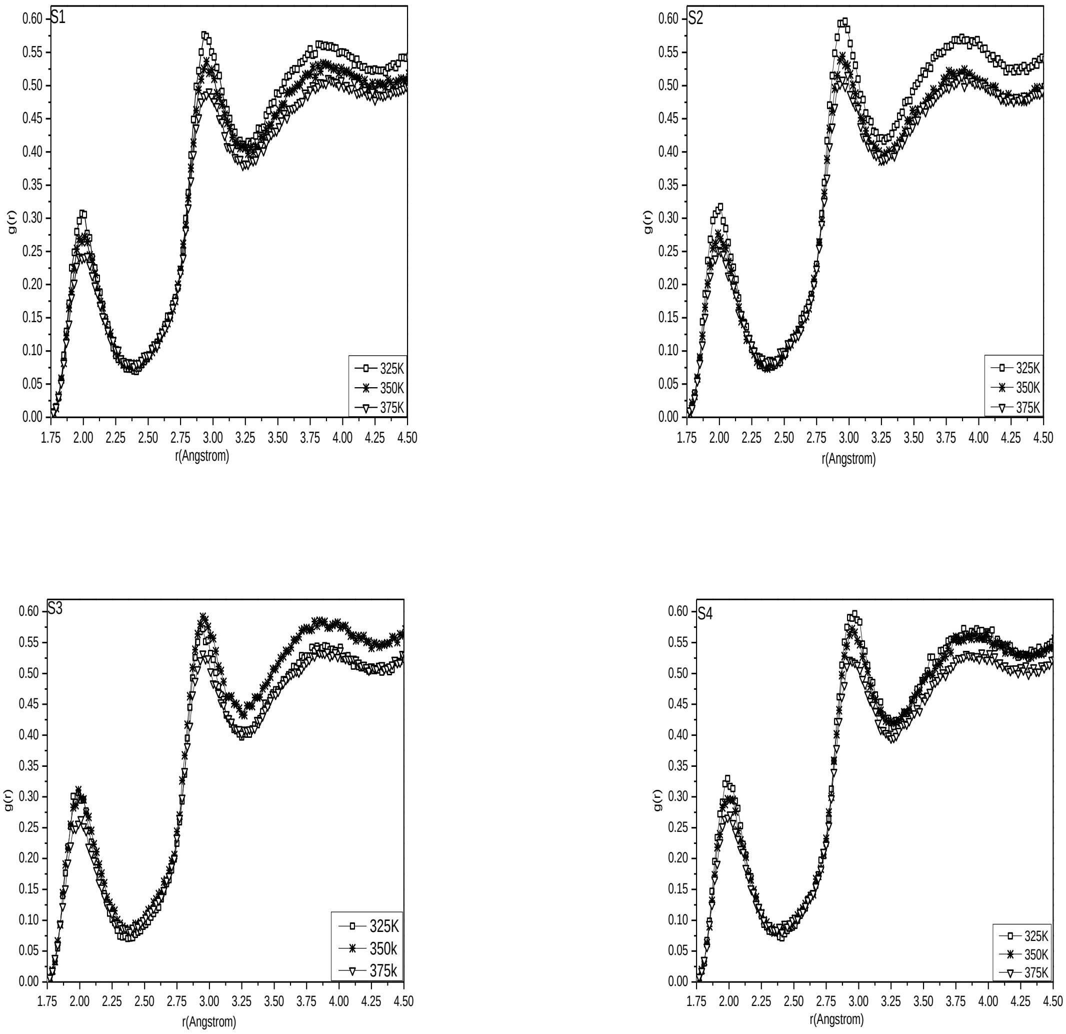

Fig. 8 Radial distribution function for microsphere and water molecules pairs in S1, S2, S3, and S4 systems at 325K, 350K, and 375K. (R denote the distance between the geometric centre of the microsphere and the oxygen of the water molecules)

From Fig. 10, both the $RDF_{O(W)-O(COOH)}$ and $RDF_{O(W)-N(NH2)}$ shows occurrence of a well-defined first peak and a weak second peak (not shown), then approaching a value of unity at longer distances (not shown). In the same system, when temperature increased, the value of first peaks of $RDF_{O(W)-N(NH2)}$ and $RDF_{O(W)-O(COOH)}$ both decreased. It also illustrate that increase of temperature weaken the hydrogen bond formed by both carboxylic group and amide group interacting with water molecular. In the same system at same temperature, the first peak of $RDF_{O(W)-O(COOH)}$ appears earlier than the first peak than $RDF_{O(W)-N(NH2)}$. Furthermore, multiple peak are observed for $RDF_{O(W)-O(COOH)}$ but $RDF_{O(W)-N(NH2)}$ only shows single peak in all four systems. The reason for these is the hydrogen bond interaction between oxygen atom in carboxylic group and hydrogen atom in water molecule are stronger than hydrogen bond between nitrogen atom in amide group and hydrogen atom in water molecules.

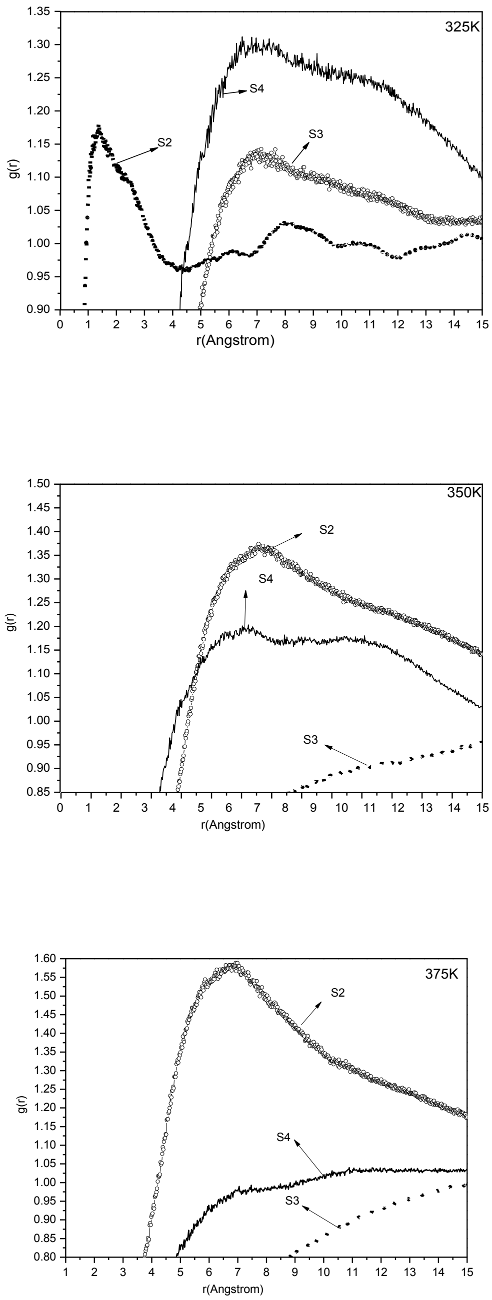

Fig. 9 Radial distribution function for microsphere-surfactant pairs in S2, S3, and S4 systems at 325K, 350K, and 375K. (R denotes the distance between the geometric centre of the microsphere and the centre of surfactant molecules).

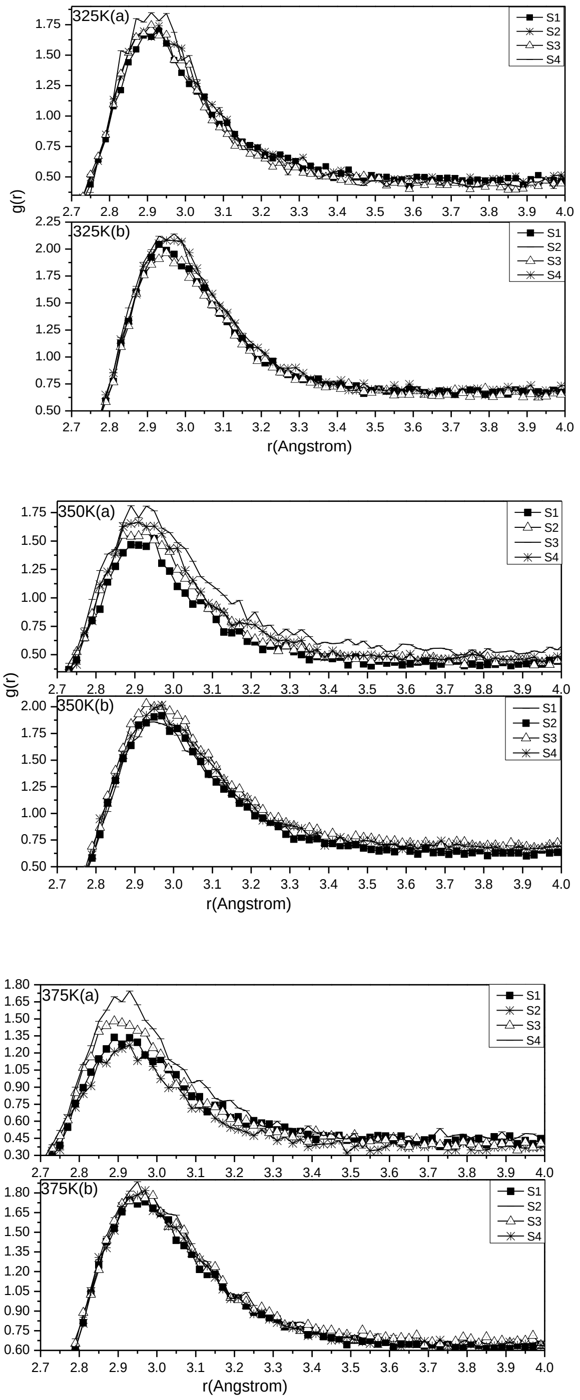

Fig. 10 Radial distribution function of carboxyl groups and amide groups from the water molecules in S1, S2, S3 and S4 systems at 325K, 350K, 375K, r denotes the distance between the oxygen atom of carboxyl group, nitrogen atom of the amide groups from oxygen of water molecules. RDF$_{O(W)-O(COOH)}$ refer to radial distribution function for carboxyl groups and water molecules are shown in panel(a), RDFO(W)-N(NH2) refer to radial distribution function for amide groups and water molecules are shown in panel (b).

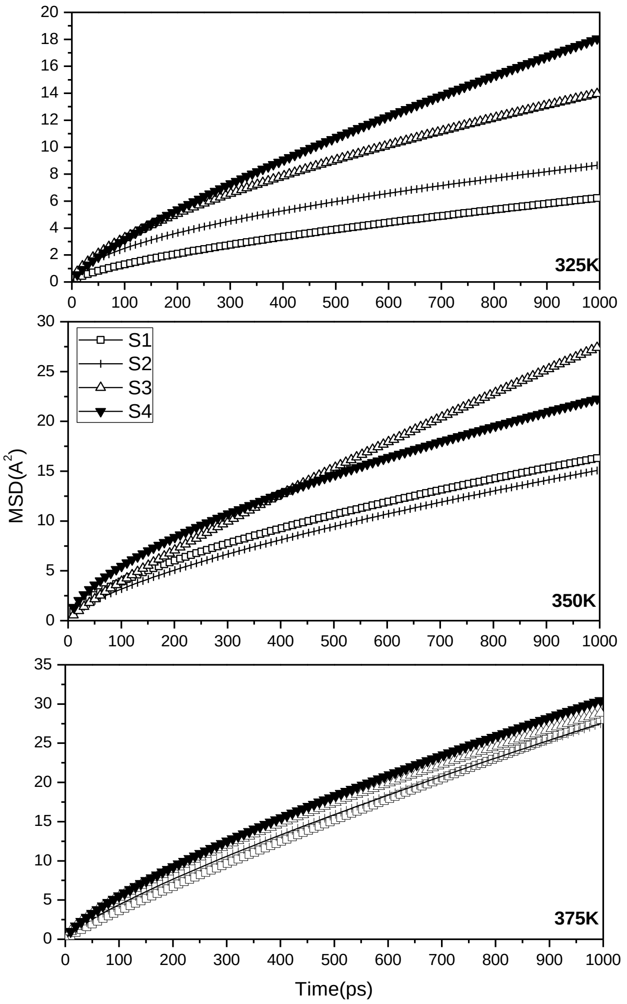

Fig.11 Mean square displacement of S1, S2, S3 and S4 system at 325K, 350K, 375K.

4.4. Mean Square Displacement of Copolymer Chains on the Surface of microsphere.

Because of the different interaction between microsphere and solutions, the chain mobility in these systems is expected to be anisotropic. For a system at equilibrium, the particles will move in accordance with the equations of motion that define the system and, in general, will tend to diffuse away from their original location. MSD of the particles with respect to their original position is obtained as the second moment of their distribution at t>0.

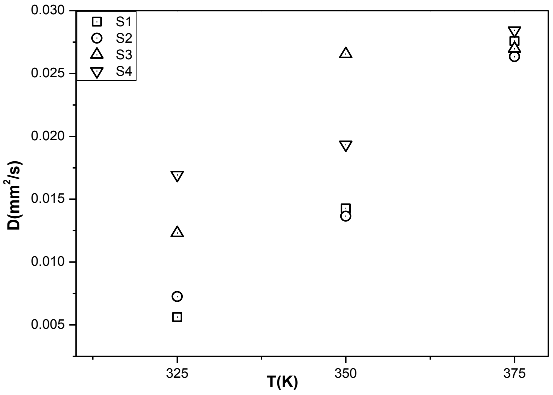

Fig.12 Diffusion coefficient of polymer chains in S1, S2, S3 and S4 system at 325K, 350K, 375K.

MSD and the diffusion coefficient (D) are calculated by the following equation:

$$\mathrm{MSD} = \lim_{t\to\infty} \frac{d}{dt} \sum_{i=1}^{N} < |r_i(t) - r_0(t)|^2 >$$

$$D = {}^{a}/_{6}$$

Where, r (t) is the centre-of-mass position vector of chains at time, and “a” denotes the slope of the best-fit line of MSD versus time.

Fig. 11 and 12 show MSD and D of copolymer chains respectively. In general, D increased as the temperature enhanced in all the 4 systems. Namely, the mobility of copolymer chains is improved with increasing temperature. But under different systems, the influence of temperature on the mobility of polymer chains are inconsistent, D of S3 system are almost no longer increase at 350K but D of S1, S2 and S4 system has a trend of liner increase with the increase of temperature. This indicated that the addition of surfactant has an effect on the mobility of polymer chains, in other words, interaction between surfactant molecule and polymer chains affect the mobility of copolymer chains. In addition, in the low temperature zone at 325K, the diffusion coefficient of these four systems have certain gap, but in the high temperature zone at 375K, the diffusion coefficients of S1, S2, S3 and S4 system have little difference. This illustrate that different solution environment has little effect on the mobility of polymer chains of microsphere at high temperature.

5. Conclusion

The microsphere of PAMAA graft nanosilica is first optimized by annealing dynamic method and obtained a reasonable structure which forming a core-cell microsphere, then the optimized microspheres in aqueous solution, SDS solution, DTAB solution and AEO solution are investigated by MD simulation using Dreiding forcefield. non-bond energy, radius of gyration of microsphere, radial distribution function for microspher-additive pairs and mean square displacement of polymer chains in these 4 different solutions are calculated in 325K, 350K and 375K respectively. Simulations show that the chains configuration of the microsphere in water solution and surfactant solution are changed due to the effect of van der Waals, hydrogen bond, coulomb interaction and hydrophobic interaction, the addition of surfactant make the polymer chains more stretched and the temperature have a great influence on the interaction between polymer chains and surfactant. With the increase of temperature, the stretched extent of polymer chains reduce in aqueous solution due to the broken hydrogen bond, in DTAB solution, and high temperature make the chains bended due to the bad thermal stability of DTAB. The stretch extent of polymer chains increased in AEO solution due to the enhanced hydrophobic effect, but influence of temperature on the structure of polymer chains in SDS solution is not obvious. Based on MSD results, the mobility of all systems increased with increase of temperature in general, but effect degree of temperature on each system are different, temperature have greater influence on mobility of S1, S3 than S2, S4 system. In addition, in the higher temperature, mobility of polymer chains in various solutions was quiet different. According to non-bond energy calculation, coulomb electrostatic energy play a leading role on structures, and the addition of surfactant increase the hydration energy, van der Waals effect and coulomb electrostatic interaction. Radial distribution function for polymer and surfactant shows that surfactant molecules are interacted with polymer chains, and stretched chains can interact with surfactant molecules uniformly. Radial distribution function for groups and water results show the hydration effect reduced with the increase of temperature.

Acknowledgements

We are grateful for support from National Natural Science Foundation of China (51304163) and China Postdoctoral Science Foundation (2014M562507XB). We also acknowledge Southwest Petroleum University and Polymer Research Institute of Sichuan University for support of this work.

References

1 V. Bounor-Legaré and P. Cassagnau, Progress in Polymer Science, 2014, **39**, 1473-1497.
2 H. Watanabe, M. Nishimura and Y. Fukui, Langmuir, 2014, **30**, 1630-1635.
3 J. T. Park, J.H. Koh, J.A. Seo, Y.S. Cho and J.H. Kim, Applied Surface Science, 2011, **257**, 8301–8306.
4 L. Zhao and Z. Lin, Advanced Materials, 2012, **24**, 4353-4368.
5 Y. Du, S. Z. Shen and K. Cai, Progress in Polymer Science, 2012, **37**, 820-841.
6 Y. Zhou, M. Cheng and X. Zhu, J. Mater. Chem. A, 2013, **1**, 11329-11334.
7 P. F. Green, Soft Matter, 2011, **7**, 7914-7926.
8 A. Jayaraman, Journal of Polymer Science Part B: Polymer Physics, 2013, **51**, 524-534.
9 X. Mu, J. Qiao and L. Qi, ACS applied materials & interfaces, 2014, **6**, 21346-21354.
10 M. Z. Rong, M. Q. Zhang and Y. X. Zheng, Polymer, 2001, **42**, 3301-3304.
11 C. J. Weng, Y. L. Chen and C. M. Chien, Electrochimica Acta, 2013, **95**, 162-169.
12 L. F. Cai, X. B. Huang and M. Z. Rong, Polymer, 2006, **47**, 7043-7050.
13 J. Liu, Y. Gao and D. Cao, Langmuir, 2011, **27**, 7926-7933.
14 L. T. Yan and X. M. Xie, Progress in Polymer Science, 2013, **38**, 369-405.
15 Z. Xu, X. Yang and Z. Yang, Nano letters, 2010, **10**, 985-991.
16 C. Wei, D. Srivastava and K. Cho, Nano Letters, 2002, **2**, 647-650.
17 H. Eslami and M. Behrouz, the Journal of Physical Chemistry C, 2014, **118**, 9841-9851.
18 R. Toth, D. J. Voorn and J. W. Handgraaf, Macromolecules, 2009, **42**, 8260-8270.
19 R. Toth, F. Santese and S.P. Pereira, Journal of Materials Chemistry, 2012, **22**, 5398-5409.
20 T. V. M. Ndoro, E. Voyiatzis and A. Ghanbari, Macromolecules, 2011, **44**, 2316-2327.
21 H. Eslami, M. Rahimi and F. Müller-Plathe, Macromolecules, 2013, **46**, 8680-8692.
22 H. Liu, M. Espe and D. A. Modarelli, J. Mater. Chem. A, 2014, **2**, 8705-8711.
23 A. F. Wells, Structural Inorganic Chemistry, Oxford Science Publications: New York, 1984.
24 S. Yang, J. Choi and M. Cho, ACS applied materials & interfaces, 2012, **4**, 4792-4799.
25 S. L. Mayo, B. D. Olafson and W. A. Goddard, 1990, **94**, 8897-8909.
26 J. E. Joes, Physical and Engineering Sciences, 1924, **106**, 463-477.
27 H. Sun, the Journal of Physical Chemistry B, 1998, **102**, 7338-7364.
28 M. P. Allen; D. J. Tildesley, Computer Simulation of Liquids, OUP, Oxford 1989.
29 H. C. Andersen, Journal of Computational Physics, 1983, **52**, 24-34.
30 H. J. C. Berendsen, J. P. M. Postma and W. F. van Gunsteren, The Journal of chemical physics, 1984, **81**, 3684-3690.
31 Ewald P P. Evaluation of optical and electrostatic lattice potentials [J]. Ann. Phys, 1921, 64: 253-287.

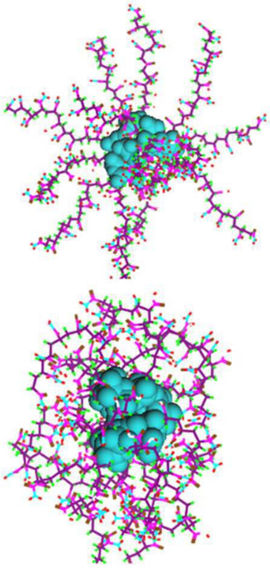

Different additives have a remarkable effect on the microstructure of polymer/inorganic core-shell microsphere in aqueous solution.